Peer-reviewed version available at Aerospace 2019, 6, 132; doi:10.3390/aerospace6120132

Article

Determination of serviceability limits of a turboshaft engine by the criterion of blade natural frequency and stall margin

Yaroslav Dvirnyk [1,2], Dmytro Pavlenko [2] and Radoslaw Przysowa [3*]

1 JSC Motor Sich, Zaporizhzhia, Ukraine; dvirnyk@gmail.com
2 National University - Zaporizhzhia Polytechnic, Zaporizhzhia, Ukraine; dvp1977dvp@gmail.com
3 Instytut Techniczny Wojsk Lotniczych, Warsaw, Poland; radoslaw.przysowa@itwl.pl
* Correspondence: radoslaw.przysowa@itwl.pl

Abstract: This paper analyses the health and performance of 12-stage axial compressor of the TV3-117VM/VMA turboshaft operated in a desert environment. The results of the dimensional control of 4,800 worn blades are analysed to model the wear process. Operational experience and numerical simulations are used to assess the effectiveness of an Inlet Particle Separator. Numerical modal analysis is performed to generate the Campbell diagram of worn blades and identify resonant blade vibration which can lead to high cycle fatigue (HCF). It is shown that the gradual loss of the stall margin over time determines the serviceability limits of compressor blades. Recommendations setting out go / no-go criteria are made to maintenance and repair organisations.

Keywords: gas-turbine performance, turboshaft, axial compressor, blade, FEM, CFD, erosion, wear, stall margin, compressor surge, brownout

1. Introduction

Long-term engine performance in adverse operating conditions is one of the main conditions for successful helicopter missions. Unlike an aeroplane, the helicopter has to hover for a long time above the ground, often raising cloud dust and causing a brownout. Therefore, the ability to conduct long-term operations at elevated dust concentrations is one of the most important features of modern helicopters. Studies on the impact of environmental particles on the efficiency of helicopter engines were already carried out during the development of the first types of helicopters [1].

The operation of a helicopter engine in a dusty environment causes contamination of the gas path [2,3]. Deposition of particles on aerofoils [4,5] and the heat exchanging surfaces of the air cooling system [6] can lead to deterioration of the aerodynamic and thermodynamic properties of these components. Moreover, given that dust particles (no matter how small they are) have abrasive properties, they also cause erosive wear of the engine components and contribute to various types of structural damage [7–9]. Erosive wear of compressor blades leads to reduction in the stall margin of the compressor, increase in the likelihood of fatigue damage of compressor blades due to changes in their natural frequencies of vibration and a decrease in the efficiency of the engine due to the wear of the gas path.

Rotating components are sensitive to mechanical damage caused by solid particles [10]. The models describing their impact and related erosive damage were proposed by many researchers, such as Finney [11], Bitter [12] and Sheldon [13], but the prediction of the actual aerofoil degradation is still difficult. The main factors affecting the magnitude of erosion consist of the angle of collision, velocity and particle size, blade surface properties, and particle concentration. Van der Walt [14] showed that the wear rate of the aerofoils is directly proportional to dust concentration. The mechanical properties of the material are also an important parameter influencing the mechanisms of erosion [15,16].

Eustyfeev [17] performed experimental and theoretical studies of compressor blades eroded by solids to determine the erosion resistance of the blade material EI-961. The limiting ratio of the particle size to their velocity of contact with the material was determined. But the experiment was performed

Preprints (www.preprints.org) | NOT PEER-REVIEWED | Posted: 4 November 2019 doi:10.20944/preprints201911.0036.v1

Peer-reviewed version available at Aerospace 2019, 6, 132; doi:10.3390/aerospace6120132

on a cut-out sample, not on a real blade, as well as on one type of material, that is EI-961 steel, while most of the blades of modern compressors are made of titanium alloy.

Batcho [18] and Singh [19] analysed loss of performance caused both by erosion and deposition. The impact of ingested particles on engine operation depends on the physical and chemical properties of the dust, its composition and concentration. Particles deposited on compressor aerofoils change their geometry and roughness, which leads to a decrease in the efficiency and consequently reduces the pressure ratio and performance of the compressor [20].

The time between overhauls (TBO) of an engine operated in a highly dusty environment is much less than that set by the manufacturer and is reduced by the erosion of the compressor blades. The statistical analysis [21] showed that erosive wear of compressor blades was the cause of 30 - 35% of the engines grounded due compressor blade damage, the largest of all causes. This is comparable to the proportion of engine removals due to foreign objects ingested from the runway during take-off (25 - 30%). The share of aviation incidents, bird ingestion, or human errors during maintenance accounts for 15 - 20%.

The aim of this study was to assess the serviceability limit of the blades of the axial compressor of a helicopter engine operating in a dusty environment. To achieve this goal, the following tasks based on the results of the dimensional control of worn blades were performed:

- establishing patterns of blade wear as a function of flight hours (FH) and dust concentration
- evaluating the increase of the natural frequency of blades by modelling the geometry of worn aerofoils over the engine operating time
- development of a methodology for modelling the flow through the axial compressor
- calculating the compressor maps describing the blades with different degrees of wear

2. Methods

In this work, the compressor blades of the TV3-117 turboshafts (Figure 1) powering the Mi-8MTV and Mi-24 helicopters helicopters in the desert environment of the Republic of Algeria are studied. The region of North Africa and the Middle East features, in addition to extreme ambient temperatures, a high concentration of dust and sand dispersing up to a height of 6000 m which is the helicopter operation zone. For example, in North Sudan, the dust concentration is $1.3\,\mathrm{g/m^3}$, and in Algeria 1.3 - $1.6\,\mathrm{g/m^3}$. The size of particles ingested into the gas path ranges from 0.01 to 2 mm.

The operation of gas-turbine engines in the regions described above, with a high content of dust and sand, inevitably leads to deterioration of engine performance [22,23]. Airborne particles may cause substantial erosive wear of compressor blades. A consequence of this is a widening of the tip clearance and a modification of the aerofoil profile - in particular, the chord length and the blade thickness appear to decrease, especially above 66% of the span (Figure 2). This leads to reduction in compressor pressure ratio and ultimately a reduction in efficiency of the entire engine.

Firstly, a statistical analysis was carried out to study the nature of compressor wear and to determine its critical components. Based on the subsequent regression analysis, patterns of wear of the blades of all compressor stages as a function of engine operation time and dust concentration were established.

The obtained patterns of the chord wear of blades of the all compressor stages were used to predict their geometry, depending on the engine operating time. This allowed for the modelling of blade vibration, simulation of the flow through the worn compressor and a determination of the serviceability limit of the blades in terms of structural integrity and the stall margin.

For the analysed engines, the observed impact of erosion on compressor performance was several times greater than deposition, due to a high dust concentration and fair inlet protection. Moreover, compressor fouling can be reversed by washing. Therefore, particle deposition is not taken into account in this work.

Preprints (www.preprints.org) | NOT PEER-REVIEWED | Posted: 4 November 2019 doi:10.20944/preprints201911.0036.v1

Peer-reviewed version available at Aerospace 2019, 6, 132; doi:10.3390/aerospace6120132

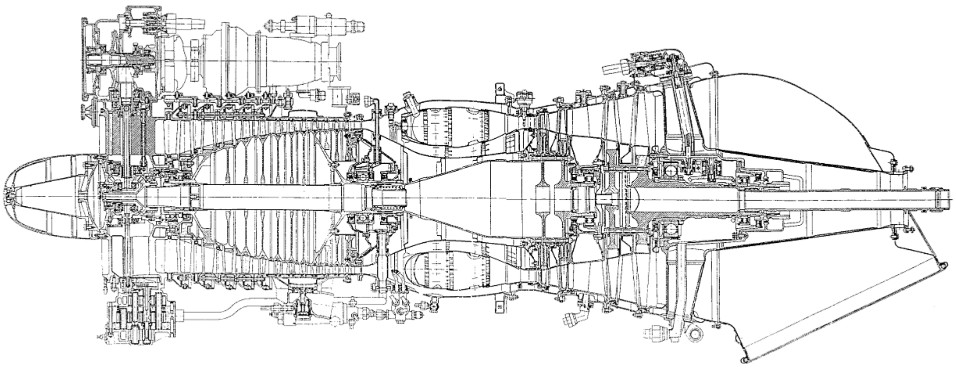

Figure 1. TV3-117 turboshaft

2.1. Blade inspection

The inspected engines were grounded and torn down for one of two reasons: either due to the chord wear of the compressor blades of the first stage in the upper part exceeding 2 mm; or, due to the performance parameters of the engine, such as the gas generator speed n_1 or the turbine inlet temperature TIT, being outside the permissible limits.

The dimensional control of blade geometry was performed by measuring the chord and the thickness of the profile at various sections as well as blade height. Ten blades were selected for the evaluation from each stage of 40 engines [24]. In total, 4,800 blades were inspected. Statistica 12 was used to analyse the results.

The inspected engines were initially divided into two categories. The first included those that were operated without a particle separator (IPS) and the second, with an IPS.

Figure 2. Blades of a compressor of a turboshaft subjected to erosive wear

2.2. Structural analysis

Compressor blades of modern turboshafts are characterised by thin profiles and relatively low stiffness, therefore forced vibration represents a notable threat to them [25,26]. The compressor blades absorb intense static and dynamic loads. When rotating under large centrifugal forces, the blades undergo deformation, which leads, in particular, to a decrease in their twist. The compressor blades vibrate due to unsteady flow forces relative to their static deformations. The distribution of dynamic stresses in blades has to be determined to ensure that they are below the fatigue limit of the material [27,28].

The erosive wear of blades has a significant impact on their strength, which is confirmed by the works of Hamed [1,29]. The properties of the blade surface and its ability to withstand erosion are one of the key factors that determine the reliability of the system, since a variety of surface irregularities can lead to stress concentration that increases the risk of high cycle fatigue (HCF) [30–33].

The main reason for the excitation of blade vibration is circumferential flow irregularity. The flow is also non-uniform in the radial direction. The frequencies of the driving forces are multiples of the

Preprints (www.preprints.org) | NOT PEER-REVIEWED | Posted: 4 November 2019 doi:10.20944/preprints201911.0036.v1

Peer-reviewed version available at Aerospace 2019, 6, 132; doi:10.3390/aerospace6120132

rotor speed (engine orders) which are equal to the number of obstacles around the circumference, e.g. the number of guide vanes and struts in the gas path. When the speed changes, a number of resonant frequencies can be excited. To predict the frequencies of resonant vibration, a modal analysis of blades and the Campbell diagram are necessary [34,35].

Vibration frequencies and operational deflection shapes can be determined with a certain degree of accuracy by numerical methods, in particular using volumetric finite element models (FEM). At present, this research method is preferred, since the complex geometry of the aerofoils is generally not amenable to the analytical method of calculating frequencies and vibration modes.

Blade geometry was measured using 3D scanning, followed by postprocessing in the CAD system ASCON KOMPAS 16.0. Geometry models of compressor blades were developed in Unigraphics NX8. Compressor blades after various periods of operation in a dusty environment were described using parameterized solid-state models. By varying blades height, chord length and thickness in the corresponding sections of the aerofoil, several variants of blade geometry were generated.

The grid models of blades, developed using the ANSYS ICEM CFD grid generator, consisted of 15 - 18 thousand hexagonal SOLID 185 elements. The calculation of the natural vibration frequencies of the blades was carried out numerically using the ANSYS 14.5 solver.

2.3. CFD model

The 3D flow calculation, with an ideal gas as the working fluid, was based on the Navier-Stokes equations and the finite element method (FEM), implemented in the ANSYS CFX solver. The mesh was developed in ANSYS Turbo Grid to model the operation of the compressor (Figure 3). A separate mesh flow model (domain) was designed for each stage (Figures 4, 5). The domains were designed taking into account the possibility of air flow to leak in the radial gap (Figure 6) by adding the interface in the blade tip. The compressor model consisted of 26 domains.

The following grid parameters were considered when building the grid:

- ATM Optimized topology ensures a high quality mesh with hexahedral elements for twisted aerofoils
- Parameter $y\pm$ size of the first wall element has a value within (80-160) units
- The ratio of the dimensions of the elements does not exceed 6.

First, the flow calculation was performed for two rotational speeds: 95% and 98%, where 1% corresponds to 195.37 rpm. Ambient air temperature of 288 K and pressure of 101.325 kPa was assumed. Each rotational speed of the compressor rotor corresponds to certain angles of variable inlet guide vanes (IGV) and guided vanes of the further four stages.

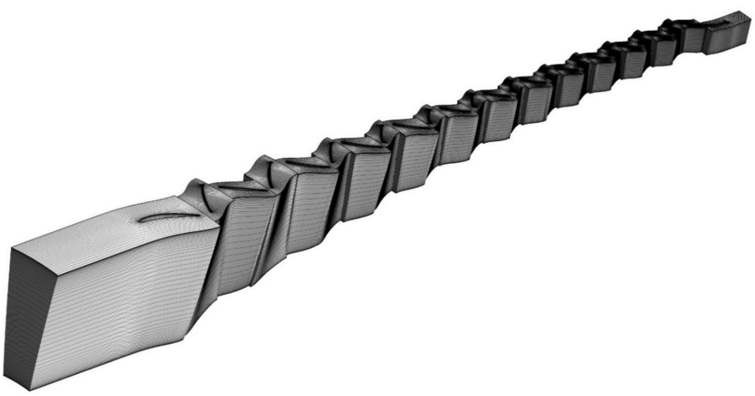

Figure 3. CFD model of the compressor

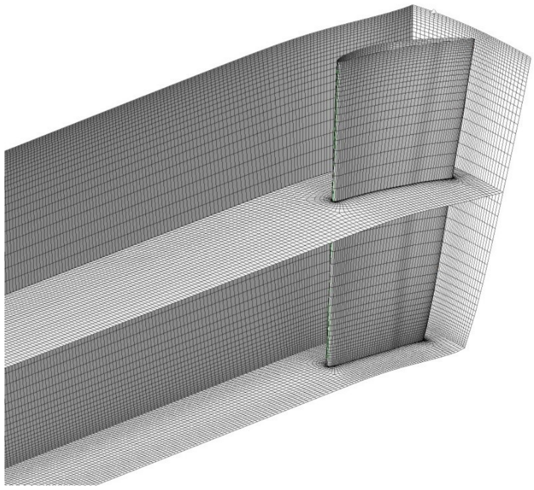

Figure 4. Mesh of inlet flow

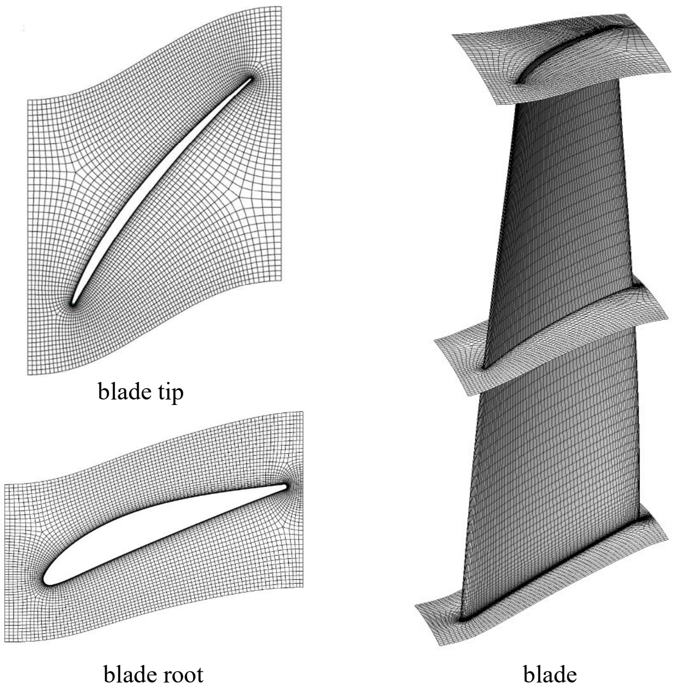

Figure 5. CFD mesh for the first stage blade

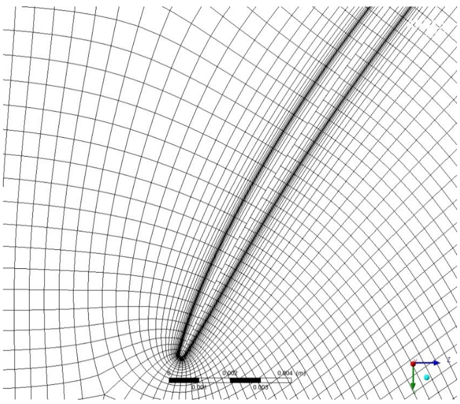

Figure 6. Mesh in the tip gap

Preprints (www.preprints.org) | NOT PEER-REVIEWED | Posted: 4 November 2019 doi:10.20944/preprints201911.0036.v1

Peer-reviewed version available at Aerospace 2019, 6, 132; doi:10.3390/aerospace6120132

To reduce the required computing power, a single blade with cyclic symmetry along the lateral boundaries of the domain was modelled for each compressor stage. Stage interfaces (Mizing-Plane) between fixed and rotating domains were defined, which allowed for interpolation between interconnected grids, taking into account the laws of mass conservation.

The choice of the turbulence model depends on the nature of the turbulent flow, the required accuracy, the available computational resources, and the time cost. The SST K-ω turbulence model of Mentera was chosen as more accurate and reliable for the class of flows with a positive pressure gradient. The residual RMS error of 1×10^{-6} was assumed as the satisfactory condition of CFD convergence and it was achieved after 600-870 iterations.

CFD results were used to estimate the compressor maps, as in another paper about this turboshaft [36]. The mass flow rate was measured at the outlet of the compressor. Each operating point corresponded to a certain mass flow, in the range from 4 to 11 kg/s.

2.4. Modelling two-phase flow through IPS

The modelling of multiphase flows presents a number of difficulties compared to single-phase flows, since it is necessary to solve the equation of mass, amount of motion and energy conservation for each phase separately. These equations are much more complicated than single-phase currents, since they have additional terms that govern the exchange of mass and energy between phases. However, due to various concomitant physical phenomena and possible changes in the flow regime, the exact value of additional members is not always known.

In order to solve these problems, we considered multiphase dispersion flows in which there is one continuous as well as one dispersion phase. The dispersed phases contained many particles distributed in a continuous phase. Euler model and ANSYS CFX software were used for modelling. The equations of mass, amount of motion and energy conservation were solved separately for each phase. In the equations of motion, the interfacial drag force and other forces observed in multiphase dispersed systems were taken into account. The calculations determined the local flow rate, temperature and volume fraction of the dispersed phase. A granulation model was used to account for particle collision, friction, and density of the particles.

To simulate two-phase flow and obtain results on the velocity of motion and distribution of dust particles in the air, the following assumption were made:

- geometric model of the separator
- concentration and chemical composition of dust
- pressure and air velocity in the separator
- flow model: two-phase
- full pressure at the inlet to the engine: 101325 Pa
- exit velocity: 150 m/s
- temperature: 288 K
- turbulence model: K-ϵ
- dust concentration at the inlet: 2 g/cm^2
- foreign particles material: quartz sand
- particle size: case 1) 10 - 50 µm, case 2) 50 - 100 µm

3. Results and discussion

3.1. Chord wear

The results of the dimensional control of the compressor blades show that the highest wear is observed at the blade tip, while a much lower wear is exhibited near the root (Figure 7). The chord wear of sections 2 - 4 can be expressed as a function of the wear of the tip section.

Preprints (www.preprints.org) | NOT PEER-REVIEWED | Posted: 4 November 2019 doi:10.20944/preprints201911.0036.v1

Peer-reviewed version available at Aerospace 2019, 6, 132; doi:10.3390/aerospace6120132

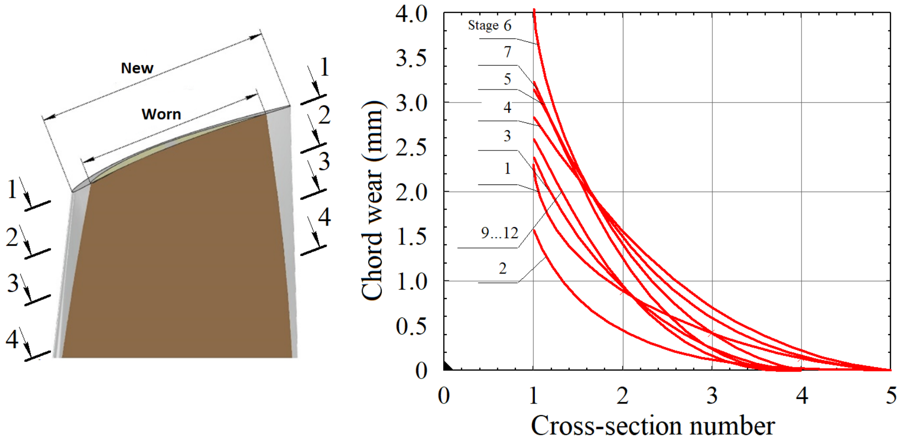

Figure 7. Chord wear of the compressor blade in specific cross-sections

Statistical analysis carried out for individual stages revealed the wear patterns caused by the design features of the compressor. Figure 8 shows the chord wear of the compressor blades of all the stages. For engines operated without IPS, the largest wear is observed for the first-stage blades while for engines operated with IPS, for the sixth stage blades.

Engines belonging to the first category, operated without IPS, were grounded in accordance with the current standards for the maximum allowable wear of the chord of the blade of the first stage of the compressor in the upper part: 2 mm. The effective TBO of the first category engines was only 150 - 200 FH, provided that nominally for this type of engine is 1500 FH.

Engines from the second category, operated with IPS, were removed from service due to their operating parameters, such as n_1 speed and turbine inlet temperature beyond the permissible limits. The effective TBO for the second category was 600 - 650 FH which indicates a partial effectiveness of the applied IPS [37].

Given the close correlation (R > 0.856) between the wear of the blades of stages 2-12, it is possible to assess the wear of the blades of each stage based on the established regression dependencies. The chord wear of the sixth stage blades is used as the independent variable. This choice is explained by the fact that, despite the obvious advantages of using the first stage for the dimensional control of blades, which are the most convenient from the point of view of monitoring and predicting remaining useful life (RUL) without removing and disassembling the engine, it does not correlate well with the wear of the remaining stages (R < 0.4).

The chord wear of the compressor stages 2-12 correlates with the wear of the sixth-stage blades and can be estimated using the linear regression.

$$c_i = a_i\, c_6 + b_i \tag{1}$$

The dependence of the chord wear on the compressor blades on the engine operating time in a dusty environment can be satisfactorily described by a second-order curve (Figure 9).

$$c_6 = (4.69 \times 10^{-6}\, t + 1.25 \times 10^{-3})\, t\, \delta \tag{2}$$

where δ is the dust concentration in g/m^3. For the analysed fleet, the average concentration δ =1.6 g/m^3 can be assumed:

$$c_6 = 7.5 \times 10^{-6} t^2 + 0.02t \tag{3}$$

Preprints (www.preprints.org) | NOT PEER-REVIEWED | Posted: 4 November 2019 doi:10.20944/preprints201911.0036.v1

Peer-reviewed version available at *Aerospace* **2019**, *6*, 132; doi:10.3390/aerospace6120132

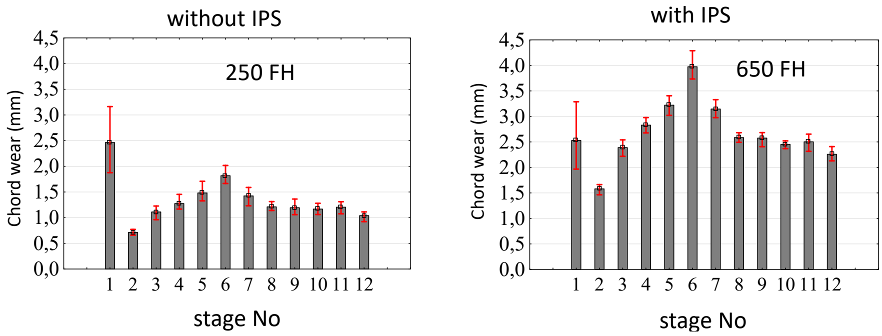

Figure 8. Average chord wear of individual compressor stages, for an engine operated without IPS or with IPS

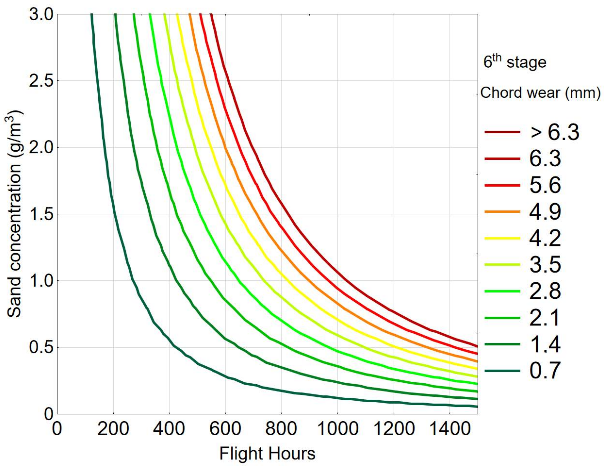

Figure 9. Chord wear of sixth-stage blades in function of flight hours

3.2. Modal analysis of blades

To assess the effect of wear on the natural frequency of the vibration, a modal analysis was performed (Figure 10). For each stage, an individual Campbell diagram was developed taking into account the nominal and worn profile of the aerofoil. Erosion significantly increases the natural frequencies of the blades. The analysis reveals several resonances excited by engine orders. Some stages were identified for which there is a risk of resonance in the operating speed range (Figure 11).

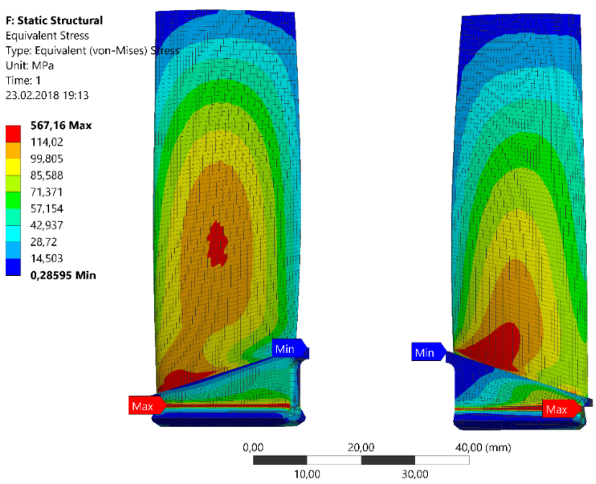

Figure 10. Modal and kinetostatic stresses of the first-stage blade with a nominal (left) and worn aerofoil (right) for $n_1 = 100\%$

Preprints (www.preprints.org) | NOT PEER-REVIEWED | Posted: 4 November 2019 doi:10.20944/preprints201911.0036.v1

Peer-reviewed version available at Aerospace 2019, 6, 132; doi:10.3390/aerospace6120132

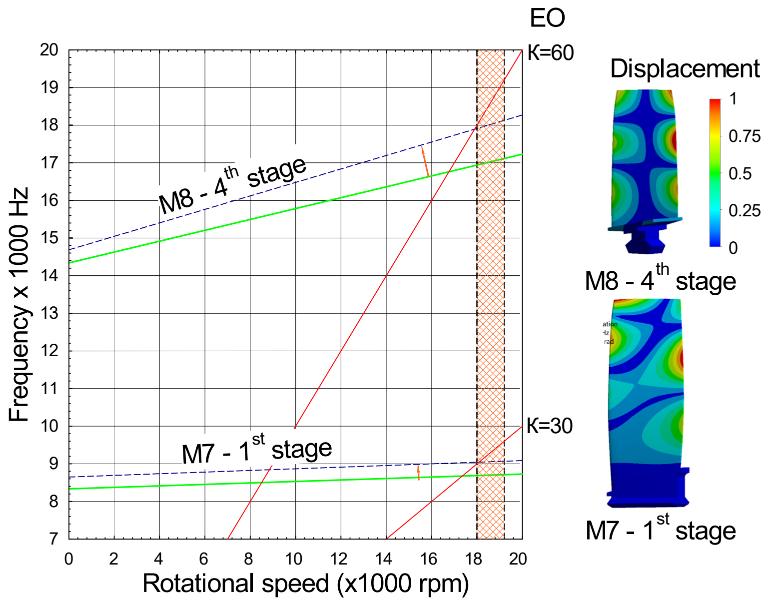

Figure 11. Impact of erosion on the Campbell diagram for critical modes and stages

Stages and the modes for which the risk of resonance is identified:

- M7 of the first stage resonates with the EO30 due to the number of the inlet guide vanes. This resonance is possible at 4 mm chord wear in the upper part
- M8 of the fourth stage resonates with the EO60 due to the number of the guide vanes of this stage. Resonance occurs when the chord wear equals 6.3 mm

3.3. Particle Separator

A particle separator cleans the air entering the engine from dust, sand, dry twigs, leaves and other foreign objects during taxiing, take-off and landing from unpaved runways or landing areas [38]. When IPS is turned on, with the engine running, hot air from the compressor enters the dust ejector nozzle. At the same time, due to centrifugal forces, part of the airflow entering the engine is pressed to the rear of the central fairing and enters the separator inlet. Most of the cleaned air passes through a separator to the engine inlet. Contaminated air, including foreign particles, passes into the dust exhaust pipe, in which a vacuum is created due to the operation of the ejector. Thus, particles are expelled into the atmosphere.

The results of modelling the speed and trajectory of foreign particles of various sizes flowing in the gas path showed that most of the particles are separated along the internal curved surface of the IPS under the action of centrifugal forces. However, experience from the operation of helicopters in a dusty environment shows that the use of this type of particle separator does not eliminate the problem of erosive wear of compressor aerofoils [37].

IPS is effective at separating large fractions of particles ranging in size from 50 to 100 µm, almost completely cleaning the air supplied to the engine compressor (Figure 12). If the particle size is relatively small - from 10 to 50 µm, about 20% of the particles enter the engine compressor bypassing the IPS separator under the influence of viscous forces following the flow. (Figure 13).

Preprints (www.preprints.org) | NOT PEER-REVIEWED | Posted: 4 November 2019 doi:10.20944/preprints201911.0036.v1
Peer-reviewed version available at Aerospace 2019, 6, 132; doi:10.3390/aerospace6120132

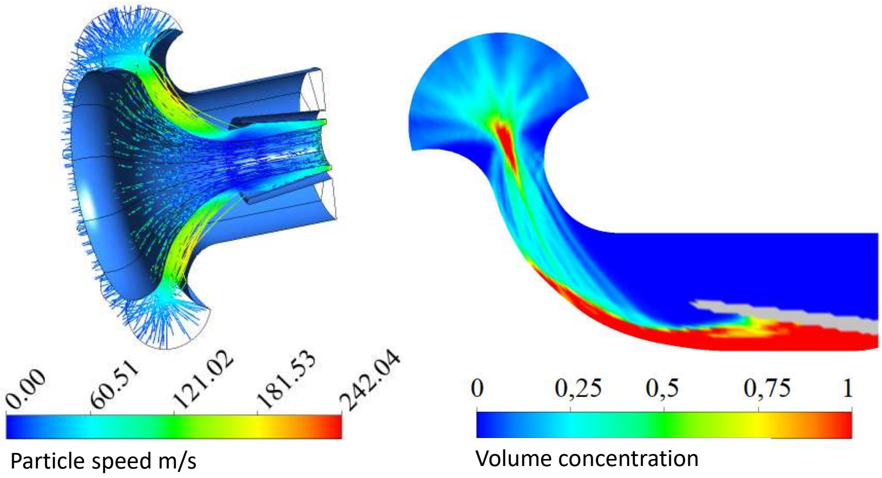

Figure 12. Velocity and concentration of large particles in the inlet of the turboshaft with IPS; particle size 50 - 100 µm

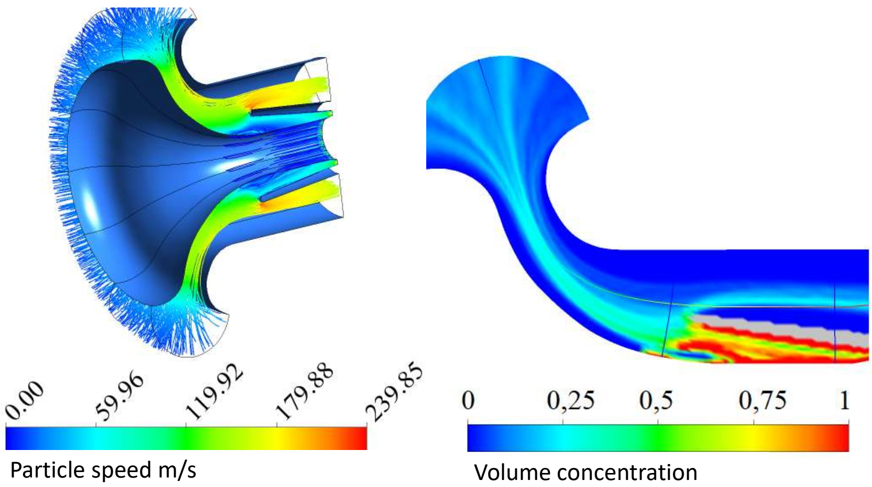

Figure 13. Velocity and concentration of small particles in the inlet of the turboshaft with IPS; particle size 10 - 50 µm

3.4. Stall margin analysis

To assess the effect of erosion on the compressor performance, the flow was calculated for the nominal (initial) geometry of the blades, as well as the geometry corresponding to the engine operating time of 200, 400, 600, and 800 FH [24].

Compressor pressure maps (Figure 14) and efficiency maps (Figure 15) calculated as a function of flight hours show that with increasing intensity of blade wear, the pressure ratio and its efficiency decreases. Consequently, the stall margin (SM) is also reduced (Figure 14). It was calculated using the following formula:

$$\mathrm{SM} = 100\% \left(\frac{\pi_{stall} / \dot{m}_{stall}}{\pi_{ss} / \dot{m}_{ss}} - 1 \right) \tag{4}$$

where π_{stall} is the pressure ratio for the stall line, and π_{ss} is the pressure ratio for the steady state line.

A decrease in the stall margin of the compressor by 15% causes the appearance of a surge during test-cell testing of TV3-117 engines. The analysis of the mass flow in the high speed region for a compressor with blades with different degrees of wear showed that due to erosive wear in the upper parts of the blades of stages 6-9, the compressor develops a stall, leading to surge. The reason for this phenomenon was a decrease in the chord of the blades and an increase in the radial clearance. For that

Preprints (www.preprints.org) | NOT PEER-REVIEWED | Posted: 4 November 2019 doi:10.20944/preprints201911.0036.v1

Peer-reviewed version available at *Aerospace* **2019**, *6*, 132; doi:10.3390/aerospace6120132

reason, the compressor operated in a dusty environment reaches its serviceability limit after 730 - 750 FH (Figure 16).

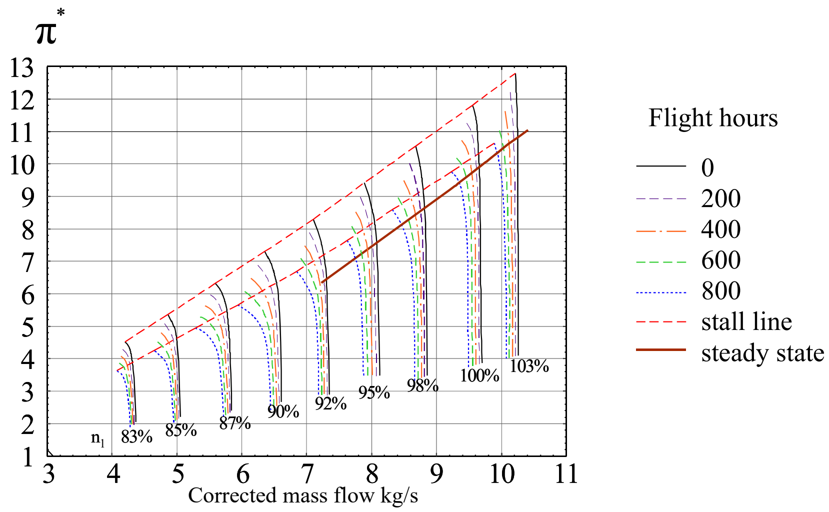

Figure 14. Dependence of the pressure compressor maps on the operating time in a dusty environment

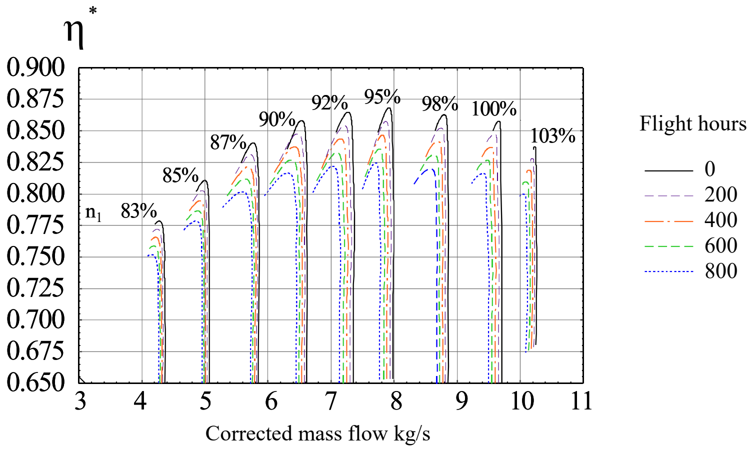

Figure 15. Compressor efficiency versus operating time in a dusty environment

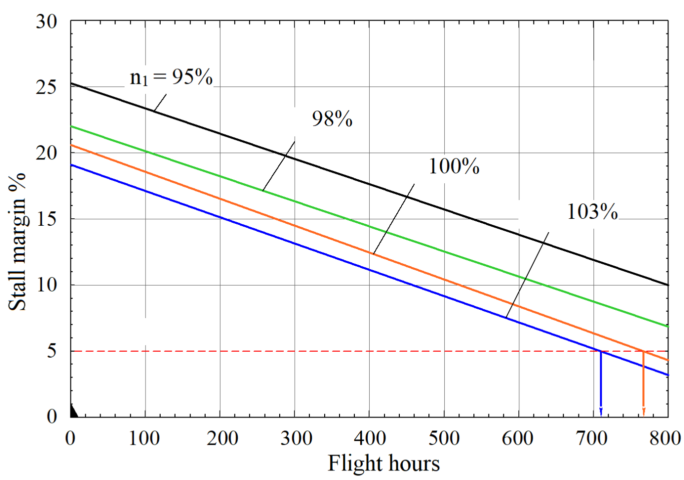

Figure 16. Stall margin of the compressor versus operating time in a dusty environment

Preprints (www.preprints.org) | NOT PEER-REVIEWED | Posted: 4 November 2019 doi:10.20944/preprints201911.0036.v1

Peer-reviewed version available at Aerospace 2019, 6, 132; doi:10.3390/aerospace6120132

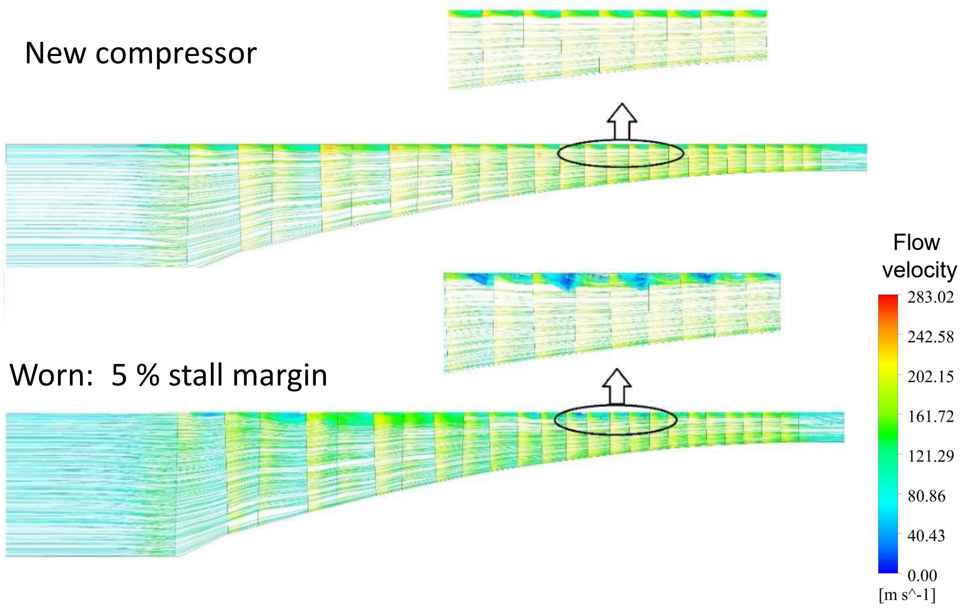

Figure 17. Flow velocity in the upper region of the flow part of the new and worn compressor

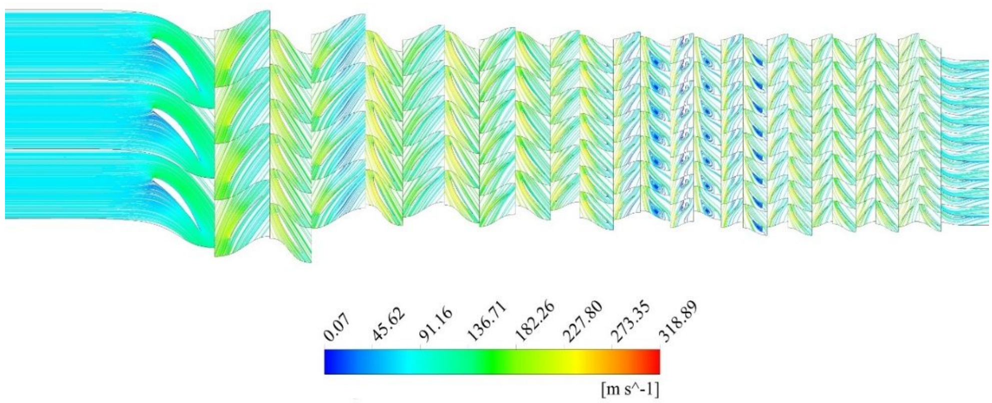

Figure 18. Flow velocity at 90% blade span

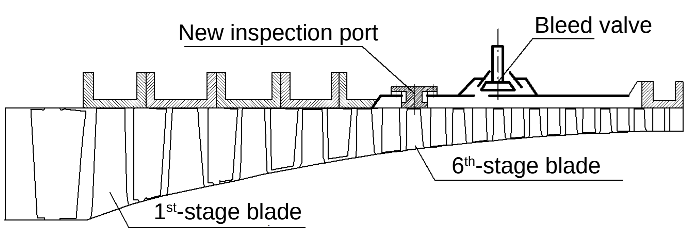

Figure 19. New slot designed to inspect the sixth stage

4. Conclusions

Based on the analysis of the geometry of the compressor blades of the TV3-117 engines operated in a dusty environment it was found that the wear of the blades of all the compressor stages occurs uniformly. When the particle separator is used, the largest wear is observed for the blades of stages 1-6.

Preprints (www.preprints.org) | NOT PEER-REVIEWED | Posted: 4 November 2019 doi:10.20944/preprints201911.0036.v1

Peer-reviewed version available at *Aerospace* **2019**, *6*, 132; doi:10.3390/aerospace6120132

It is also established that there is a close correlation between the wear of the blades of the sixth stage and the stages 2-12.

An original method was developed to assess the influence of erosive wear of the blades and vanes on the compressor performance by modelling three-dimensional flow for various degrees of wear on the blades of all stages. The methodology for measuring the chord wear of the blades, calculating the natural frequencies of vibration taking into account the aerofoil wear, numerical calculation of the compressor flow and analysing the onset of stall, the use of which, in combination with established patterns of chord wear over engine operating time allowed for the assessment of the serviceability limits of the blades.

On the basis of a modal analysis of compressor blades with different operating times, the dependency of blade vibration frequency on the chord wear for all the stages was established. It was found that when the chord of the first-stage blades is worn more than 4 mm, the M7EO30 resonance can occur. Similarly, chord wear of the forth-stage blades higher than 5.1 mm causes M8EO60 vibration. The HCF risk for the remaining stages is negligible.

The values of the maximum permissible chord wear of the blades of all stages are determined by the criterion of stall margin of the TV3-117 turboshaft. The chord wear of the sixth-stage blades equal 6.19 mm is critical because it is accompanied by a decrease in the stall margin of the compressor by 15-17% which indicates the appearance of a permanent stall at 770-790 FH. An additional slot for the optical inspection of the sixth stage was designed to allow for field maintenance (Figure 19).

The standards applicable today determine the maximum chord wear of blade in its upper section at the level of 2 mm, regardless of the use of particle separators. The criteria established in terms of natural vibration frequency and the margin of stall margin allow for increasing the time between overhauls (TBO) by 200 FH. The defined serviceability limits of the blades enable helicopter users to significantly reduce operating costs by extending the RUL of the engines operated in a desert environment.

Author Contributions: Y. Dvirnyk and D. Pavlenko conceived and designed the research; Y.D. processed and analysed the data; Y.D. and D.P developed FEM and CFD models; D.P. and R. Przysowa verified and evaluated the results. Y.D. and R.P. drew conclusions and produced the paper.

Funding: This research received no external funding

Acknowledgments: This publication was prepared within the framework of the AERO-UA project, which has received funding from the European Union's Horizon 2020 research and innovation program under grant agreement No 724034.

Conflicts of Interest: The authors declare no conflict of interest. JSC Motor Sich had no role in the design, execution, interpretation, or writing the study. The views, information, or opinions expressed herein are solely those of the authors and do not necessarily represent the position of any organisation.

References

1. Hamed, A.A.; Tabakoff, W.; Rivir, R.B.; Das, K.; Arora, P. Turbine blade surface deterioration by erosion. *Journal of Turbomachinery* **2005**. doi:10.1115/1.1860376.
2. Szczepankowski, A.; Szymczak, J.; Przysowa, R. The Effect of a Dusty Environment upon Performance and Operating Parameters of Aircraft Gas Turbine Engines. *STO-MP-AVT-272 Impact of Volcanic Ash Clouds on Military Operations* **2017**, pp. 1–13. doi:10.14339/STO-MP-AVT-272-06-PDF.
3. Przysowa, R.; Gawron, B.; Kulaszka, A.; Placha-Hetman, K. Polish experience from the operation of helicopters under harsh conditions. *Journal of KONBIN* **2018**, *48*, 263–300. doi:10.2478/jok-2018-0056.
4. Doring, F.; Staudacher, S.; Koch, C.; Weißschuh, M. Modeling particle deposition effects in aircraft engine compressors. *Journal of Turbomachinery* **2017**, *139*. doi:10.1115/1.4035072.
5. Doring, F.; Staudacher, S.; Koch, C. Predicting the Temporal Progression of Aircraft Engine Compressor Performance Deterioration due to Particle Deposition. *Proceedings of the ASME Turbo Expo 2017: Turbomachinery Technical Conference and Exposition* **2017**. doi:10.1115/GT2017-63544.
6. Bojdo, N.; Filippone, A. A Simple Model to Assess the Role of Dust Composition and Size on Deposition in Rotorcraft Engines. *Aerospace* **2019**, *6*, 44. doi:10.3390/aerospace6040044.

7. Abdullin, B.R.; Akmaletdinov, R.G.; Gumerov, X.S.; Nigmatullin, R.R. K issledovaniyu raboty GTD v zapylennoj atmosfere [Research of gas turbine engine operation in dust-filled atmosphere]. *Vestnik Samarskogo gosudarstvennogo aehrokosmicheskogo universiteta* **2014**, pp. 95–102.
8. Kramchenkov, E. Issledovanie ehrozionnogo iznashivaniya materialov [Study of erosive wear of materials]. PhD thesis, Gubkin Russian State University of Oil and Gas, Moscow, 1995.
9. Borkova, A.N. Erozionnaya stojkost aviacionnyx materialov pri soudarenii s tverdymi (pylevymi) chasticami [Erosion resistance of aviation materials in collision with solid (dust) particles]. PhD thesis, All-Russian Institute Of Aviation Materials, Moscow, 2006.
10. *Gas Turbine Engine Environmental Particulate Foreign Object Damage [EP-FOD]*; Vol. STO-TR-AVT-250, The NATO Scientific and Technology Organization, 2019. doi:10.14339/STO-TR-AVT-250.
11. Finnie, I.; Stevick, G.R.; Ridgely, J.R. The influence of impingement angle on the erosion of ductile metals by angular abrasive particles. *Wear* **1992**. doi:10.1016/0043-1648(92)90206-N.
12. Bitter, J.G. A study of erosion phenomena. Part II. *Wear* **1963**. doi:10.1016/0043-1648(63)90073-5.
13. Sheldon, G.L.; Kanhere, A. An investigation of impingement erosion using single particles. *Wear* **1972**. doi:10.1016/0043-1648(72)90257-8.
14. van der Walt, J.P.; Nurick, A. Erosion of Dust-Filtered Helicopter Turbine Engines Part I: Basic Theoretical Considerations. *Journal of Aircraft* **1995**, *32*, 106–111. doi:10.2514/3.56919.
15. Finnie, I. Some observations on the erosion of ductile metals. *Wear* **1972**. doi:10.1016/0043-1648(72)90444-9.
16. Khodak, M.O.; Vishnevskij, O.A. Eksperimentalni viprobuvannya ta prognozuvannya xarakteristik abrazivnoi znosostoijkosti materialiv aviacijnix GTD [Experimental tests and prediction of the abrasion resistance characteristics of materials of aviation gas-turbine engines]. *Aviacionno-kosmicheskaya texnika i texnologiya* **2006**, p. 114–123.
17. Evstifeev, A.; Kazarinov, N.; Petrov, Y.; Witek, L.; Bednarz, A. Experimental and theoretical analysis of solid particle erosion of a steel compressor blade based on incubation time concept. *Engineering Failure Analysis* **2018**. doi:10.1016/j.engfailanal.2018.01.006.
18. Batcho, P.F.; Moller, J.C.; Padova, C.; Dunn, M.G. Interpretation of gas turbine response due to dust ingestion. *Journal of Engineering for Gas Turbines and Power* **1987**. doi:10.1115/1.3240046.
19. Singh, D.; Hamed, A.L.; Tabakoff, W. Simulation of performance deterioration in eroded compressors. *ASME 1996 International Gas Turbine and Aeroengine Congress and Exhibition* **1996**. doi:10.1115/96-GT-422.
20. Koch, C.C.; Smith, L.H. Loss sources and magnitudes in axial-flow compressors. *Journal of Engineering for Gas Turbines and Power* **1976**. doi:10.1115/1.3446202.
21. Shpilev, K. *Jekspluatacija letatelnyh apparatov v gorno-pustynnoj mestnosti [Operation of aircraft in the mountain-desert area]*; Voennoe izdatelstvo: Moscow, 1991; p. 224.
22. Tabakoff, W.; Hamed, A.; Wenglarz, R. Particulate flows, turbomachinery erosion and performance deterioration. *Von Karman Lecture Series* **1988**, *89*, 24–27.
23. Grigorev, V.; Zrelov, V.; Ignatkin, J.; Kuzmichev, V.; Ponomarev, B.; Shahmatov, E. *Vertoletnye gazoturbinnye dvigateli [Helicopter gas turbine engines]*; Mashinostroenie: Moscow, 2007; p. 491.
24. Pavlenko, D.; Dvirnyk, Y. Zakonomernosti iznashivanija rabochih lopatok kompressora vertoletnyh dvigatelej, jekspluatirujushhihsja v uslovijah zapylennoj atmosfery [The laws of wear of the compressor rotor blades of the helicopter engines that are operated under the dust conditions]. *Visnik dvigunobuduvannja* **2016**, pp. 42–51.
25. Vorobev, Y.; Romanenko, V. Analiz kolebanij lopatochnogo apparata kompressora GTD" [Analysis of vibrations of gas turbine compressor blading]. *Aviacionno-Kosmicheskaya Tehnika i Tehnologija* **2013**, pp. 55–59.
26. Rzadkowski, R.; Gnesin, V.; Kolodyazhnaya, L.; Kubitz, L. Unsteady Forces Acting on the Rotor Blades in the Turbine Stage in 3D Viscous Flow in Nominal and Off-Design Regimes. *Journal of Vibration Engineering and Technologies* **2014**, *2*, 3–9.
27. Witek, L. Crack propagation analysis of mechanically damaged compressor blades subjected to high cycle fatigue. *Engineering Failure Analysis* **2011**. doi:10.1016/j.engfailanal.2011.03.003.
28. Witek, L. Crack Growth Simulation in the Compressor Blade Subjected to Vibration Using Boundary Element Method. *Key Engineering Materials* **2014**, *598*, 261–268. doi:10.4028/www.scientific.net/KEM.598.261.

29. Hamed, A.; Tabakoff, W. Experimental and numerical simulations of the effects of ingested particles in gas turbine engines. *AGARD Conference Proceeding* **1994**.
30. Itoga, H.; Tokaji, K.; Nakajima, M.; Ko, H.N. Effect of surface roughness on step-wise S-N characteristics in high strength steel. *International Journal of Fatigue* **2003**. doi:10.1016/S0142-1123(02)00166-4.
31. Murakami, Y.; Tsutsumi, K.; Fujishima, M. Quantitative evaluation of effect of surface roughness on fatigue strength. *Nippon Kikai Gakkai Ronbunshu, A Hen/Transactions of the Japan Society of Mechanical Engineers, Part A* **1996**. doi:10.1299/kikaia.62.1124.
32. Dyblenko, Y.M.; Selivanov, K.S.; Valiev, R.R.; Skryabin, I.V. Issledovanie gazoabrazivnogo iznosa obrazcov iz titanovogo splava VT-6 s nanostrukturirovannymi zashhitnymi pokrytiyami [Investigation of gas-abrasive wear of VT-6 titanium alloy samples with nanostructured protective coatings]. *Vestnik Ufimskogo gosudarstvennogo aviacionnogo texnicheskogo universiteta* **2011**, *15*, 83–86.
33. Ivchenko, D.; Shtanko, P. Ob ustalostnom mexanizme gazoabrazivnoj erozii detalej gazovozdushnogo trakta vertoletnyx GTD [On the fatigue mechanism of gas-abrasive erosion of parts of the gas-air duct of a helicopter gas turbine engine]. *Visnik dvigunobuduvannya* **2009**.
34. Batailly, A.; Legrand, M.; Cartraud, P.; Pierre, C. Assessment of reduced models for the detection of modal interaction through rotor stator contacts. *Journal of Sound and Vibration* **2010**, *329*, 5546–5562. doi:10.1016/j.jsv.2010.07.018.
35. Ma, H.; Wang, D.; Tai, X.; Wen, B. Vibration response analysis of blade-disk dovetail structure under blade tip rubbing condition. *Journal of Vibration and Control* **2017**, *23*, 252–271. doi:10.1177/1077546315575835.
36. Marakueva, O. Aerodynamic design and optimization of blade configuration in an inlet stage of an aircraft engine compressor. *29th Congress of the International Council of the Aeronautical Sciences* **2014**.
37. Dvirnyk, Y.; Pavlenko, D. Zakonomernosti techenija dvuhfaznogo potoka vo vhodnom ustrojstve vertoletnyh GTD" [Laws of multiphase flow behavior in the inlet of a helicopter engine]. *Aviacionno-Kosmicheskaya Tehnika i Tehnologija* **2017**, pp. 30–37.
38. Filippone, A.; Bojdo, N. Turboshaft engine air particle separation. *Progress in Aerospace Sciences* **2010**, *46*, 224–245. doi:10.1016/j.paerosci.2010.02.001.